Available online at www.sciencedirect.com
SCIENCE DIRECT
Journal of Power Sources 155 (2006) 66–71
JOURNAL OF POWER SOURCES
www.elsevier.com/locate/jpowsour

Short communication

Investigation on the influence of channel geometries on PEMFC performance

J. Scholta *, G. Escher, W. Zhang, L. Küppers, L. Jörissen, W. Lehnert

Zentrum für Sonnenenergie- und Wasserstoff-Forschung, GB 3: Elektrochemische Energiespeicherung und -wandlung, Helmholtzstr. 8, D-89081 Ulm, Germany

Received 4 February 2004; accepted 9 May 2005
Available online 1 September 2005

Abstract

The performance of PEM fuel cells depends significantly on an appropriate flow field design. In this work, an investigation on the influence of channel geometries on stack performance has been carried out. A parallel flow field design was developed to widely eliminate the influence of other flow field design parameters, e.g. degree of parallelization and gas crossover effects at the turning points of the gas channels. Starting from a basic design, channel as well as rib dimensions were varied and their influence on stack performance were studied. An optimum between 0.7 and 1 mm was found for either channel or for rib widths. For wider dimensions, the influence on mass transport (ribs) or lateral conductivity (channels) has been found to become significant. For very small dimensions, the manufacturing effort becomes unacceptably high (ribs) and the probability of channel clogging by formation of water droplets increases. In general, narrow channel dimensions are preferred for high current densities, whereas wider dimensions are better at low current densities.

Keywords: Fuel cell; PEMFC; Flow field design; Rib and channel geometry; Cell performance

1. Introduction

PEM fuel cell stacks having an active area of 100 cm^2 and a length up to 50 cells resulting in a power of 1.4 kW have been built and operated successfully since 2001 at ZSW. A power density of up to 0.3 W cm^{-2} has been obtained. However, it is well-known, that also the degree of fuel and air utilization is of great importance to the system efficiency. Despite showing acceptable power characteristic, the utilization of hydrogen (0.35–0.7) and air (0.15–0.3) were not satisfactory. Therefore, an investigation on the influence on flow direction, flow field geometry and channel geometries has been started having the objective of improved flow field design leading to better performance. In addition to general design improvements for the flow field and operating conditions of ZSW 100 cm^2 stacks which are reported elsewhere [1], the influence of channel geometries on stack performance has been studied in this work. There are already data on this subject reported in the literature, e.g. [2]. Also, investigations of non-conventional fractal geometries are given, e.g. [3]. Since there was no superior performance of fractal geometries reported compared to serpentine or parallel flow fields, this investigation was limited to conventional designs, specially to the influence of channel and rib dimensions on the PEFC cell performance. The results published in the literature indicate that dimensions less than 1 mm for both channel and ribs could be advantageous. However, the published data are limited to a channel width of 1 mm, and the variation of rib widths is given in steps of 0.5 mm only. The same restrictions are valid for [4] where results on the modeling of gas diffusion layers (GDL) are reported. Therefore, it was of interest to find out whether channel and rib dimensions ranging from 1.5 mm to less than 1 mm could contribute to improved cell performance.

* Corresponding author. Tel.: +49 731 9530 206; fax: +49 731 9530 666.
E-mail address: joachim.scholta@zsw-bw.de (J. Scholta).
URL: http://www.zsw-bw.de.

0378-7753/$ – see front matter © 2005 Elsevier B.V. All rights reserved.
doi:10.1016/j.jpowsour.2005.05.099

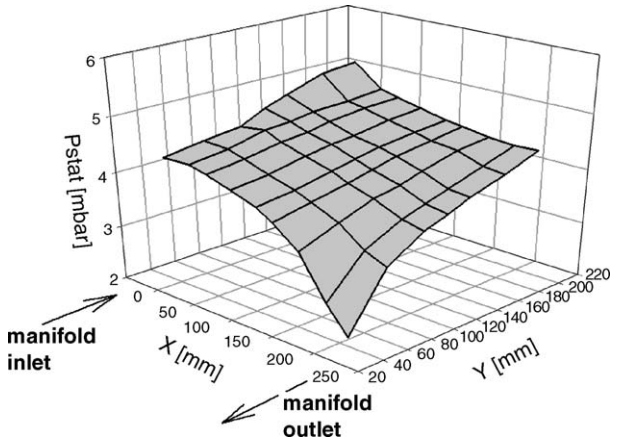

Fig. 1. Measured pressure drop in a pattern flow field.

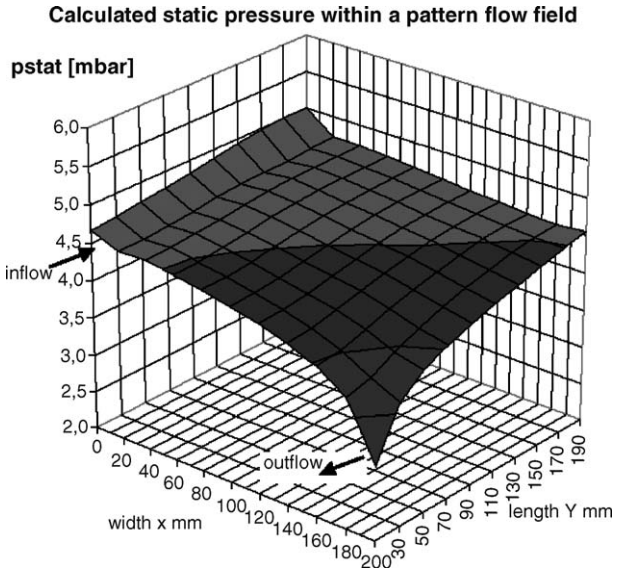

Fig. 2. Calculated pressure drop in the pattern flow field.

2. Experimental procedures

Using the basic layout of the ZSW 100 cm^2 cell design, a parallel flow field including optimized inlet and outlet areas was designed which should guarantee an almost even flow rate throughout all channels. The flow field design process was accompanied by commonly used CFD-modeling using FLUENT^{TM} software. In doing so, first approach was to verify experimental results by CFD-calculations. A measured distribution of static pressure inside a pattern flow field model of a PEM fuel cell with an active area of 400 cm^2 was the basis of comparison to CFD-results [5]. The original geometry was meshed and calculations were carried out using the standard k–ε turbulence model. At the same operating parameters as the experiments the inlet flow consists of air at ambient temperature of 20 °C and a flux of 5.7 $m^3\,h^{-1}$. Both plots (Figs. 1 and 2) show a good correlation in general behavior as well as in terms of absolute values. That means significant information can be obtained by CFD. (Slight differences in view occur due to different origins of the coordinate systems).

The air flow rate for the flow field model of the 100 cm^2 cell was set equivalent to a cell current of 50 A at an air utilization of 25%. Pressure and velocity was investigated for different inlet and outlet distribution zones with the aim to obtain an equalized flow distribution over the main area using a parallel flow field with different channel and rib dimensions. For these calculations, it was not necessary to include media conversion, because the total molar flow rate change between the cathode inlet and outlet is less than 6%. As a result, the influence of other flow field design parameters, e.g. degree of parallelization or pressure drop along the channels could be eliminated to a great extent.

Using 1 mm for channels and ribs as the basic design, channel as well as rib dimensions were varied experimentally in the range from 0.5 and 1.5 mm (Table 1).

Numerous short stacks (three cell units) were built and tested. Commercially available MEAs (GORE 5620) and GDLs (SGL 10BB) were used. The basic stack design is described in [1].

2.1. Test bench

The cell performance was determined using a test bench developed at ZSW in cooperation with hydrogen-systems. The layout is given in [6].

The test bench allows measurement and recording of all relevant parameters (stack and single cell voltages, current, temperatures and pressures). Moreover, high frequency resistance (HFR) data at a frequency of 1 kHz can be recorded online in order to assess the degree of cell humidification and to determine the contribution of cell construction (e.g. GDL compression, channel and rib dimensions). Gas humidification is achieved by passing the premixed reactant gases through a heated and isolated bubbler.

Table 1
Flow field design parameters for the test samples

	Stack number									
	"0333"	"0334"	"0335"	"0336"	"0337"	"0347"	"0348"	"0349"	"0350"	"0351"
Channel width (mm)	1.5	1.0	0.8	0.6	0.5	1.0	1.0	0.5	0.5	0.5
Rib width (mm)	1.0	1.0	1.0	1.0	1.0	1.5	0.8	0.8	0.65	0.5

2.2. Test procedures

The stacks were tested using pure hydrogen and air. Operating conditions were as follows:

T_{Stack} = 55–60 °C, ambient outlet pressure, dry anode gas, cathode inlet dew point 45 °C. Hydrogen utilization 70%, air utilization 25%.

I–U curves were recorded for all samples. The hold time for the individual data points was 30 min.

3. Results and discussion

For all investigations, counter flow between the gaseous media was selected. The cells were positioned as such, that no flow direction opposite to the direction of gravity occurred in order to avoid artefacts caused by droplets not being purged out due to gravity reasons.

3.1. Flow field design

The inlet zone of the flow field has been varied starting from a simple and symmetric pattern geometry concerning the pattern dimensions and distribution including a variation of the in- and outlet channel positions. The resulting gas distribution has been simulated numerically in order to obtain an almost equal gas flow rate distribution through all channels located in the central part of the flow field. For this simulation, the flow field design showing the lowest pressure drop was selected for optimization of the inlet and outlet areas since this situation is posing the largest constraints concerning homogeneity of the gas distribution along the *y*-length of the cell. The basic geometry of the gas flow field is visualized in Fig. 3. The calculated flow distribution (lowest pressure drop case) is shown in Fig. 4.

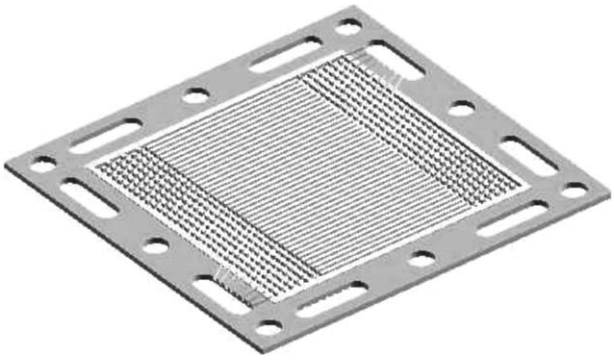

Fig. 3. Bipolar plate with flow field used for testing series.

According to the intended experimental investigations the velocity distribution was calculated at a cell air flow rate of 1 l min^{-1} equivalent to a current of 30 A at 50% utilization. As a result for the selected flow field even in the worst case (equivalent to lowest pressure drop along the channels) the ratio between the standard deviation and the average of channel gas flow rates is less than 11.1%.

3.2. CFD-calculations on oxygen distrubution at a single channel–rib system

It is well-known, that the flow field design influences not only the cell resistance but also the mass transport of gases and liquids. In addition to the experimental investigations reported below, a CFD-study on the oxygen concentration profile for a single channel–rib GDL system was performed using the FLUENT^{TM} software to investigate the influence of channel depth and rib width on the oxygen concentration profile. The flow rates for the single channel were calculated from a stack with 130 cm^2 active area and a parallel flow field without serpentines and external manifold as it is used

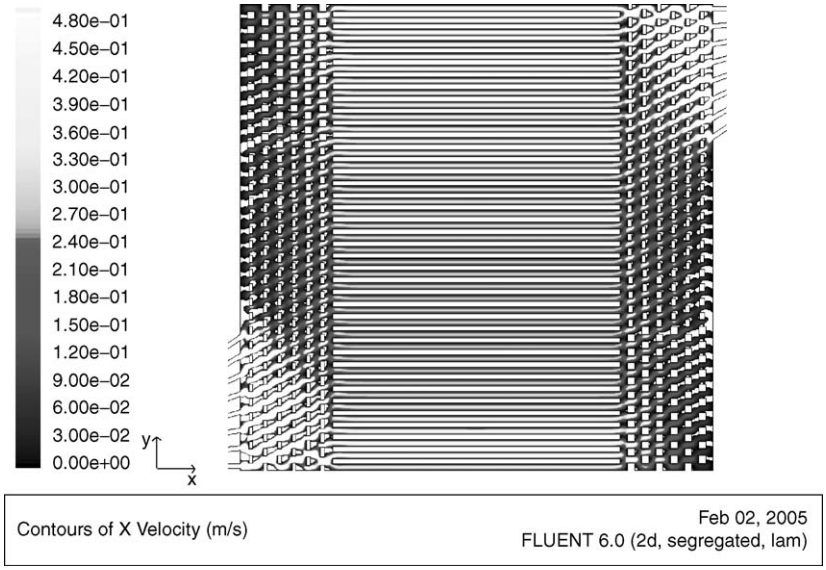

Fig. 4. CFD-calculated gas flow velocity distribution with flow field used for testing series (inlet: left, outlet: right).

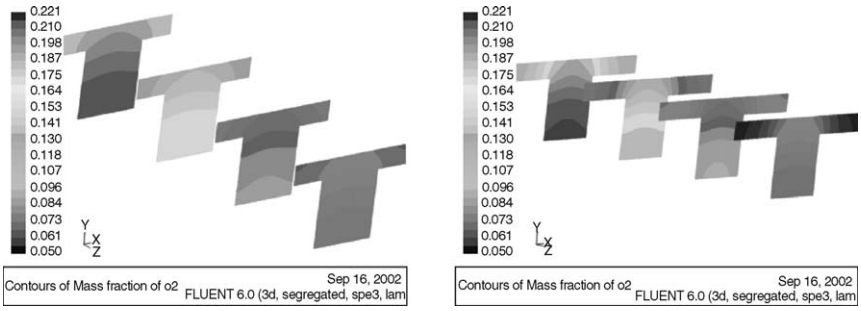

Fig. 5. O_2-concentration profile at a single model channel (1 mm × 1 mm) with a 1 and 2 mm rib.

for low air pressure systems. The current density was set to 0.4 A cm^{-2} at following operating conditions: temperature of the cell and the air was set to 60 °C having a dewpoint temperature at the inlet of 40 °C, that means a RH value of about 37.5%. The gas diffusion layer thickness was set to 0.27 mm and the air permeability to 1.76×10^{-11} m^2 according to [7]. The reaction layer was set to 0.03 mm and the overall channel length to 103 mm. Fig. 5 shows the resulting concentration profiles at an oxygen utilization of 50%. From those profiles, two conclusions can be drawn. First, a channel depth of more than 1.5 mm for a parallel flow field leads to significant amounts of "wasted" oxygen because of the setup of a *y*-concentration profile within the channel. Second, the oxygen concentration significantly drops over the rib (*x*-direction) at a rib width of 2 mm. For that reason, the rib variation was limited to 1.5 mm or less.

The results compare well with results presented in the literature [8,9].

3.3. Cell performance

Fig. 6 shows the *I–U* curves for the first series of measurements where the rib width was fixed at 1.0 mm and the channel width has been varied from 0.5 to 1.5 mm.

The comparison of current voltage curves clearly show that the sample having 1.5 mm channel width is performing lower than the rest of the test stacks. Specially, at current densities above 0.7 A cm^{-2}, at least one of the cell voltage levels fell below the limit of 300 mV, such that the experiment has been stopped in order to avoid problems caused by cell reversal. The samples having channel widths of lower or equal to 1 mm only showed smaller differences in performance: at low current densities the samples having a smaller channel width seem to perform lower, whereas at current densities above 0.6 A cm^{-2}, the samples having a channel width of less than 0.8 mm shows the highest cell voltage. An investigation of cell resistances showed that most of this effect can be attributed to a decreasing cell resistance. After *IR* correction, all cell voltages at 1.0 A cm^{-2} were within a 40 mV band. A more detailed discussion of cell resistance will follow later. In a second series, the effects of a variation of rib widths using a constant channel width of 0.5 mm have been investigated.

Fig. 7 shows the *I–U* curves for the second series of measurement where the channel width was left fixed at 0.5 mm and the rib width varying between 0.5 and 1.0 mm.

In general, the coincidence between rib width and cell performance turned out to be less sensitive as it was observed for the channel diameter variation. In this case, the curve with a rib width of 1.0 mm shows the best performance at high current densities, followed by the curve recorded with 0.5 mm channel width. The curves recorded with a rib width of 0.65 and 0.8 mm perform significantly lower at current densities of 0.7 A cm^{-2} or more. Summarizing, using a channel width of

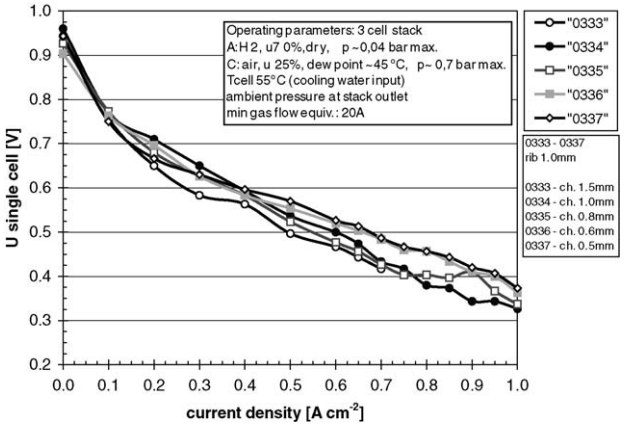

Fig. 6. *I–U* curves for samples with varying channel width and a rib width of 1.0 mm.

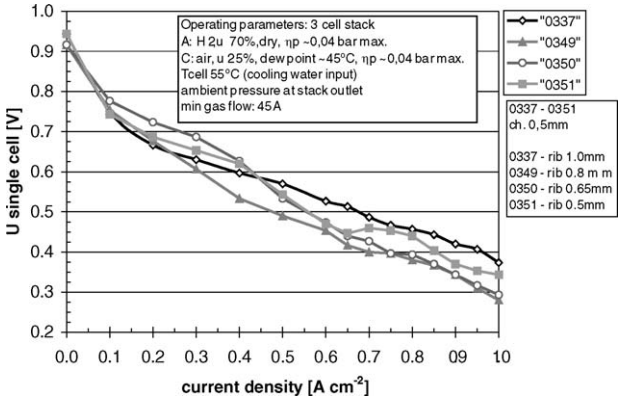

Fig. 7. *I–U* curves for samples with varying rib width and a channel width of 0.5 mm.

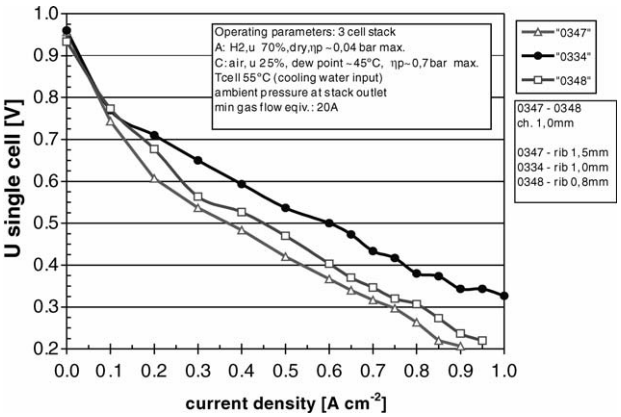

Fig. 8. *I–U* curves for samples with varying rib width.

0.5 mm, no obvious tendency in varying the rib width between 0.5 and 1.0 mm could be observed.

In a third series, the effects of a variation of rib widths using a constant channel width of 1.0 mm have been investigated. Fig. 8 shows the corresponding variation of the rib width from 0.8 to 1.5 mm using a channel width of 1.0 mm. In this case, the cell having a rib with of 1.0 mm shows the best performance compared to the data obtained applying a rib width of 1.5 and 0.8 mm.

From the data presented, it becomes obvious, that a channel and a rib diameter of 1.5 mm (or greater) is not beneficial, if higher current densities are required. These results confirm the data obtained from the CFD-study reported above. According to the CFD-study, a significant improvement of cell voltage is expected when reducing the rib width from 1.5 to 1.0 mm. For rib widths lower than 1.0 mm no more significant influence of the rib width on mass transport is predicted, which would correspond to only insignificant differences in predicted cell voltage, as it was observed in the experiment.

Therefore, for the rest of the data set, the interpretation becomes more complicated. Specially, the cells using a rib width of 1 mm turned out to perform well, independent of the channel diameters (0.5 and 1 mm). Therefore, the influence of small rib widths (between 0.5 and 1.0 mm diameter) could not be completely clarified: stack 0351 (rib 0.5 mm, channel 0.5 mm) showed a comparable performance to stack 0337 (rib 1.0 mm, channel 0.5 mm), whereas stack 0349 (rib 0.8 mm, channel 0.5 mm) showed an inferior performance. On the other hand, there may be some side effects caused by other experimental conditions, such that a more detailed analysis of the data is useful. One parameter which could lead to a further insight is the channel/rib ratio. In Figs. 9 and 10, the rib to channel ratio is given referring to the inner cell area which was varied throughout the experiments. The gas distribution zones in the inlet and outlet areas were not varied and therefore, did not tamper the observed dependencies throughout the experiments performed.

In general, a high rib to channel ratio turns out to correlate well with a low cell resistance and, in consequence also with a high cell voltage at 0.7 A cm^{-2}. The best performing stacks (0337, 0336 and 0351) are possessing a rib to channel ratio between 1 and 2. Moreover, all channel or rib widths

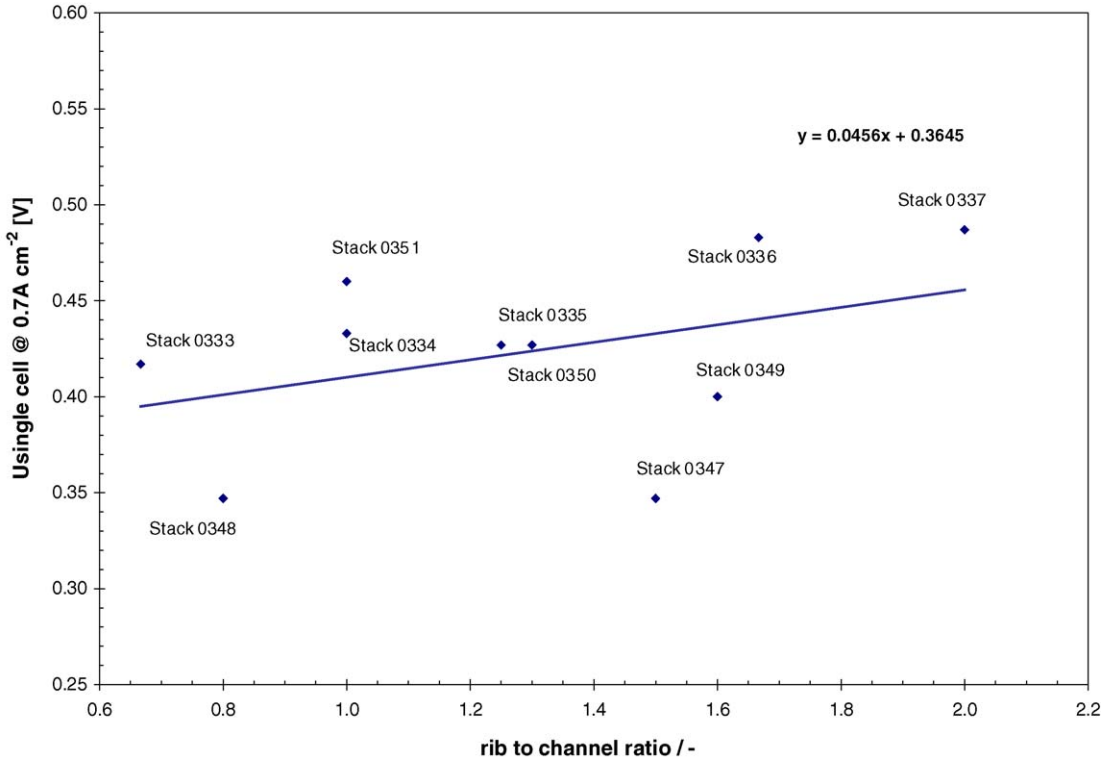

Fig. 9. Cell voltages at 0.7 A cm^{-2} dependent on rib to channel ratio.

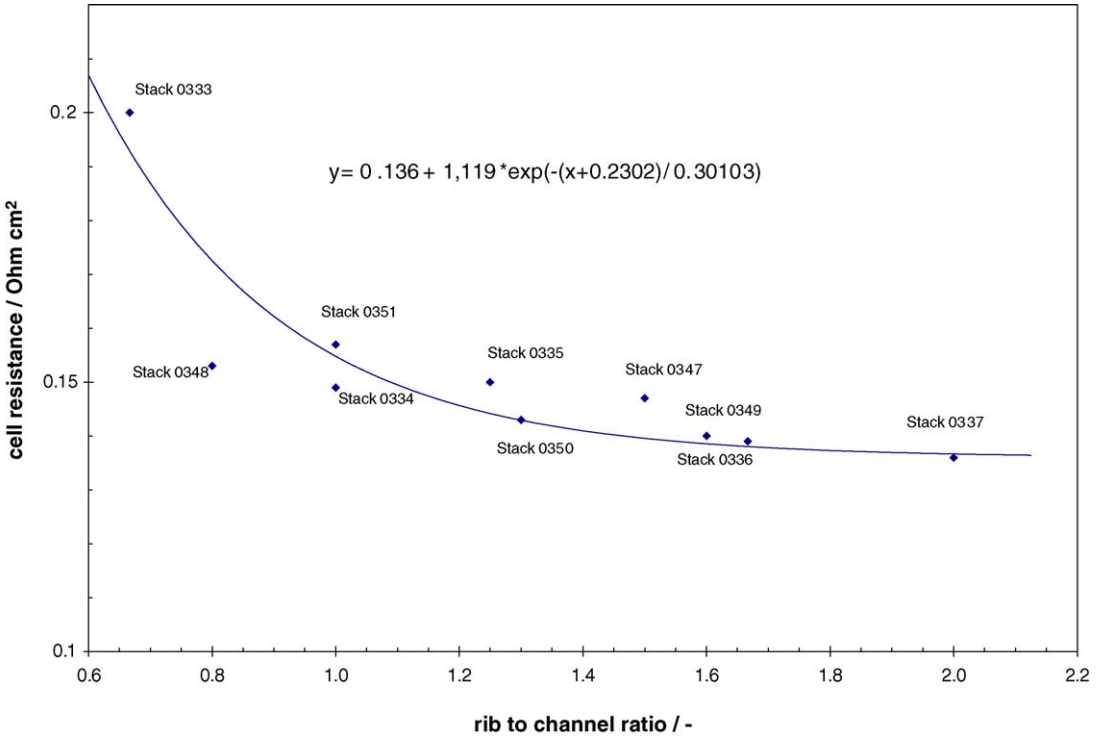

Fig. 10. Ohmic cell resistance dependent on rib to channel ratio at 0.5 A cm^{-2}.

for a good performing cell were found to be between 0.5 and 1 mm.

4. Summary and conclusion

Summarizing the results, a negative correlation between cell resistance and rib to channel ratio could be shown. In most cases, a corresponding positive correlation exists between the cell voltage at 0.7 A cm^{-2} and the rib to channel ratio for a range from 0.67 to 2. An optimum dimension between 0.5 and 1 mm was found as well for channel as for rib widths, if combined with a rib to channel ratio ≥ 1. For wider dimensions, the influence on mass transport (ribs) or lateral conductivity (channels) becomes significant. For very small dimensions, the manufacturing effort becomes unnecessarily high (ribs) and the danger of channel clogging by water droplets is increasing. Therefore, channel and rib dimensions between 0.7 and 1 mm were identified as an optimum under the operating conditions considered. In general, small dimensions are preferred for high current densities, whereas higher dimensions are better for low current densities.

The tests performed are supporting the findings on variations of the cell design reported in [1] and allow to adapt further designs to the specific performance requirements of the application.

References

[1] J. Scholta, et al., J. Power Sources 155 (2006) 60–65.
[2] Tae-Hyun Yang, Lee Won, Hye-Mi Jung, Young-Gi Yoon, Jung-Sun Park, Kim Chang, Optimization of channel dimensions in gas distributor for polymer electrolyte membrane fuel cell, in: Proceedings of the 2nd European PEFC Forum, vol. 1, Luzern, CH, June 30–July 4, 2003. Oberrohrdorf: European Fuel Cell Forum, 2003, pp. 239–244. ISBN 3-905592-13-4.
[3] K. Tüber, A. Oedegaard, M. Hermann, C. Hebling, Investigation of fractal flow-fields in portable proton exchange membrane and direct methanol fuel cells, J. Power Sources 131 (2004) 175–181.
[4] K.T. Jeng, S.F. Lee, G.F. Tsai, C.H. Wang, Oxygen mass transfer in PEM fuel cell gas diffusion layers, J. Power Sources 138 (2004) 41–50.
[5] Ch. König, Measuring of current density distribution in a model of a low temperature fuel cell (ger.), Diploma Thesis, Fachhochschule Aachen, Abteilung Jülich, 1998.
[6] J. Scholta, N. Berg, P. Wilde, L. Jörissen, J. Garche, Development and performance of a 10 kW PEMFC stack, J. Power Sources 127 (2004) 206–212.
[7] Hongtan Liu, Tianhong Zhou, Numerical simulation of performance of PEM fuel cells, in: Proceedings of the 2nd International Conference on Computational Heat and Mass Transfer, Federal University of Rio de Janeiro, Brazil, October 22–26, 2001.
[8] T. Berning, N. Djilali, Three-dimensional computational analysis of transport phenomena in a PEM fuel cell—a parametric study, J. Power Sources 124 (2003) 440–452.
[9] S. Dutta, S. Shimpalee, J.W. van Zee, Three-dimensional numerical simulation of straight channel PEM fuel cells, J. Appl. Electrochem. 30 (2000) 135–146.